

Progressive Homeostatic and Plastic Prompt Tuning for Audio-Visual Multi-Task Incremental Learning

Jiong Yin^{1,2*} Liang Li^{2 †} Jiehua Zhang³ Yuhang Gao¹ Chenggang Yan¹ Xichun Sheng⁴

¹Hangzhou Dianzi University ²Institute of Computing Technology, Chinese Academy of Sciences

³Xi'an Jiaotong University ⁴Macao Polytechnic University

{jiong.yin, yuhangao, cgyan}@hdu.edu.cn liang.li@ict.ac.cn jiehua.zhang@stu.xjtu.edu.cn p2314922@mpu.edu.mo

Abstract

Audio-visual multi-task incremental learning aims to continuously learn from multiple audio-visual tasks without the need for joint training on all tasks. The challenge of the problem is how to preserve the old task knowledge while facilitating the learning of new task with previous experiences. To address these challenges, we introduce a three-stage Progressive Homeostatic and Plastic audio-visual prompt (PHP) method. In the shallow phase, we design the task-shared modality aggregating adapter to foster cross-task and cross-modal audio-visual representation learning to enhance shared understanding between tasks. In the middle phase, we propose the task-specific modality-shared dynamic generating adapter, which constructs prompts that are tailored to individual tasks while remaining general across modalities, which balances the model's ability to retain knowledge against forgetting with its potential for versatile multi-task transferability. In the deep phase, we introduce the task-specific modality-independent prompts to further refine the understand ability by targeting individual information for each task and modality. By incorporating these three phases, PHP retains task-specific prompts while adapting shared parameters for new tasks to effectively balance knowledge sharing and specificity. Our method achieves SOTA performance in different orders of four tasks (AVE, AVVP, AVS and AVQA). Our code can be available at <https://github.com/ENJOY-Yin-jiong/PHP>.

1. Introduction

Visual and auditory perception form the core of human understanding of the world. Audio-visual multi-task learning attracts significant research interest for integrating audio-visual cues to address various tasks. However, due to the dynamic nature of the real world, once a multi-task model

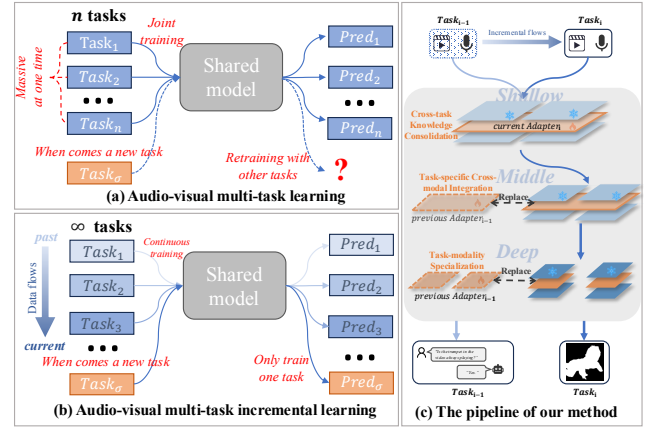


Figure 1. (a) **Audio-visual multi-task learning** allows simultaneous training on various audio and video tasks. But, the model may require retraining when a new task emerges. (b) **Audio-visual multi-task incremental learning** is able to address new tasks more flexibly while maintaining the memory of previous tasks. (c) **The pipeline of our method.**

trained uniformly is deployed, it often struggles to update continuously to acquire new knowledge, while also fulfilling new task requirements as illustrated in Fig 1 (a).

Audio-visual multi-task incremental learning aims to conduct continuous learning within audio-visual task streams without the need for simultaneous training on all tasks. An incremental learning strategy can greatly enhance the flexibility of multi-task models and enable them to quickly adapt to new tasks based on shared knowledge, as shown in Fig 1 (b). However, this approach faces the critical challenge of catastrophic forgetting, where new knowledge overwrites existing representations, causing significant performance decline on previously learned tasks.

Previous works in incremental learning have made significant progress in mitigating catastrophic forgetting. Some methods maintain memory of old tasks through parameter regularization [1, 24, 29, 78], while others rely on data replay [3–6, 14, 43, 44, 64] to revisit past knowledge.

*This work is done during the intern in VIPL group, ICT, CAS.

[†]Corresponding author

Recently, prompt-based methods [9, 21, 22, 51, 60–62] show promising potential by introducing a small number of trainable prompt parameters to adapt to new tasks, avoiding large-scale parameter updates and data storage. However, these methods primarily focus on single-modality scenarios and do not fully address audio-visual specific challenges.

Extending incremental learning to audio-visual multi-task scenarios introduces fundamental challenges beyond traditional single-modality settings: 1) *Balancing interference and knowledge sharing between tasks*. Sharing knowledge across tasks boosts individual learning but may cause interference between different tasks. Additionally, over-sharing due to task differences may exacerbate the catastrophic forgetting issue during incremental learning. 2) *Balancing the preservation of modality specificity and the integration of modality generality*. During audio-visual multi-task learning, the model benefits from mastering general representations across audio and visual modalities, which reveals intrinsic connections and improves its transfer ability. However, there exists a fundamental trade-off between cross-modal fusion and modality-specific information preservation, which can impact performance on tasks requiring detailed single-modality features. For example, the AVE task requires precise localization within each modality separately.

Inspired by the knowledge consolidation pathway observed in continual pre-trained models, where semantic circuits evolve from deep conceptual abstraction to shallow representation refinement [41], we introduce a novel Progressive Homeostatic and Plastic audio-visual prompt (PHP) method to tackle incremental forgetting issue and boost knowledge sharing with a three-stage manner. The proposed framework operates through three hierarchically organized phases: (a) cross-task knowledge consolidation at shallow layers, which transitions into (b) task-specific cross-modal integration in middle layers, ultimately culminating in (c) task-modality specialization at deep layers. In the shallow phase, the Task-shared Modality Aggregating (TMA) adapter creates the universal audio-visual representations through various cross-modal fusions. This foundational stage maximizes knowledge sharing by establishing task-agnostic correspondences critical for subsequent adaptations. In the middle stage, the Task-specific Modality-shared Dynamic Generating (TMDG) adapter enhances audio-visual representations using a prompt pool to improve perception. It then selects instance-level prompts to customize audio-video fusion for each task’s specific needs. At the deep stage, Task-specific Modality-Independent (TMI) prompts operate in isolation for each task and modality, ensuring the preservation of modality-specific details while excavating profound representations tailored to individual tasks. This reinforces the model’s resilience against the forgetting of information and strength-

ens its overall performance.

The main contributions of this paper as follows:

- We propose a Progressive Homeostatic and Plastic (PHP) audio-visual prompting framework that enables incremental learning for dynamic audio-visual task streams.
- We design a task-shared modality aggregating adapter in shallow layers that learns universal audio-visual representations through complementary attention mechanisms.
- We introduce a hierarchical prompting strategy combining task-specific modality-shared and modality-independent prompts to balance knowledge preservation and task adaptation.
- Extensive experiments on four audio-visual tasks (AVE, AVVP, AVS and AVQA) demonstrate that our method achieves state-of-the-art performance in both knowledge preservation and transfer capability.

2. Related Work

Deep learning’s development has propelled significant advancements in the field of computer vision [8, 19, 30, 42, 55, 66, 67, 69–71, 74, 75, 79–81, 86] and multi-modal learning [34, 56, 68, 83–85].

2.1. Audio-visual Understanding

Audio-visual understanding tasks focus on learning the correspondence between audio and visual modalities from videos to achieve multi-modal perception. This has led to advancements in a range of audio-visual tasks, such as audio-visual event localization [31, 52, 53, 58, 65], audio-visual parsing [16, 32, 40, 54, 63], audio-visual question answer [25–27, 37], audio-visual spatialization [17, 33, 87]. In this work, we explore the transferrable representations progressively, incrementally engaging with various audio-visual tasks. It is more challenging than the single task above as forgetting and transferability should be considered.

2.2. Incremental Learning

Incremental learning aims to continuously integrate new knowledge without compromising the integrity of previously learned information, thereby maintaining a robust and adaptable representation over time. Its major challenge is the catastrophic forgetting problem [39], which occurs when the model’s performance on previously learned tasks significantly degrades as it learns new tasks. To reduce the issue, architecture-based methods often extract features from multiple layers [23, 38, 48] or extend models [28, 46, 47, 49, 72, 76], but the effectiveness of these models is severely limited due to the complexity of the extended models. Regularization-based methods [1, 24, 29, 78] impose constraints on loss functions to preserve old knowledge, but their effectiveness depends on the relationship between tasks, limiting their use in complex scenarios. Rehearsal-based methods maintain a subset of past data to revisit old

knowledge [3–6, 14, 43, 44, 64], but they are sensitive to data selection [3–5, 20, 64, 77] and face issues with privacy and memory [50].

2.3. Prompt Tuning for Incremental Learning

Recent works [2, 9, 10, 12, 18, 21, 22, 35, 36, 51, 57, 60–62, 73] in incremental learning show that prompt tuning is an efficient method for adapting models by training only new inputs and reusing existing knowledge without full re-training. L2P [62], as the pioneer method of prompt tuning in incremental learning, introduces prompts as trainable parameters in continual learning, bypassing the need for rehearsal by selecting from a prompt pool. DualPrompt [61] innovates by dividing the prompt pool into task-agnostic and task-specific subsets for more efficient learning. Similar to DualPrompt, S-Prompt [60] independently learns task-specific prompts to reduce catastrophic forgetting through separate tuning strategies. However, this leads to an increase in prompts with the number of tasks, with selection based on a one-hot indexing method. As an improvement, PC [9] generates more expressive prompt representations by creating instance-specific prompts from a predefined prompt codebook. In this work, we conduct audio-video multi-task incremental learning through three stages to simultaneously enhance the model’s anti-forgetting capability and multi-task transferability.

3. Proposed Approach

3.1. Overview

Audio-visual multi-task incremental learning aims to conduct continuous learning in the data stream of audio-visual tasks. This allows the model to adapt to changing data in real-time and continuously emerge new tasks. The challenge lies in: 1) Balancing interference between tasks and knowledge sharing. 2) Balancing the preservation of modality specificity and the integration of modality generality.

Our framework utilizes CLIP [45] and CLAP [15] as the backbone with three complementary components operating at different network depths: In the shallow stage, we employ a Task-shared Modality Aggregating (TMA) adapter to learn universal audio-visual representations that can benefit multiple tasks. This stage emphasizes the extraction of fundamental cross-modal correspondences, which serve as shared foundational features across diverse audio-visual tasks. In the middle stage, The Task-specific Modality-shared Dynamic Generating (TMDG) adapter is designed to balance task specificity and modality sharing. This component generates adaptive prompts that help maintain task-specific knowledge while enabling cross-modal feature integration. In the deep stage, we develop Task-specific Modality-independent (TMI) prompts to preserve the unique characteristics of each modality and task. This

ensures that critical task-specific and modality-specific information is retained during incremental learning.

3.2. Problem Formulation

Assuming $\mathcal{D} = \{\mathcal{D}_1, \mathcal{D}_2, \dots, \mathcal{D}_T\}$ as a sequence of tasks with T incremental tasks, where t -th audio-visual task $\mathcal{D}_t = \{(a_i^t, v_i^t, y_i^t)\}_{i=1}^{N_t}$ contains tuples of audio-visual pair $a_i^t \in \mathcal{A}^t$ and $v_i^t \in \mathcal{V}^t$ and the corresponding ground-truth labels $y_i^t \in \mathcal{Y}^t$. The audio-visual multi-task incremental learning is defined to train a single model $f_\theta : (\mathcal{A}, \mathcal{V}) \rightarrow \mathcal{Y}$ with θ parameters to handle the T different audio-visual tasks. During the training and inferring phase, the current task is available, which allows the model to update the suitable prediction module and generate appropriate outputs.

3.3. Task-shared Modality Aggregating Adapter

Zhang *et al.* [82] indicates that the shallow stage of a model learns the local structure and feature representation of the data. At the deeper stage of a model, it is capable of learning more complex discriminative information and latent concepts to address different tasks more effectively. Inspired by this, we first propose the Task-shared Modality Aggregating (TMA) adapter to enable the model to prioritize learning cross-task, cross-modal audio-video representations at the shallow stage.

Overall, drawing insights by DG-SCT [13], TMA adapter consists of channel attention, spatial attention, and temporal attention fusion, which together facilitate the fusion of audio-video multi-modal data from multiple perspectives. Specifically, channel attention enables bidirectional feature refinement between modalities by identifying semantically related channel patterns. For an input video feature v^t and audio feature a^t , the audio-to-video channel attention map M_{ac}^t is computed through global statistics aggregation and channel projection:

$$M_{vc}^t = \sigma(W_v \cdot \delta_v(\Phi_a(a^t))) \in \mathbb{R}^{C_v \times 1}, \quad (1)$$

where $\Phi_a(\cdot)$ denotes global average pooling over spatial-temporal audio dimensions, $\delta_v(\cdot)$ projects pooled features to video channels, and W_v implements learnable spatial weighting. Conversely, the video-to-audio channel adaptation follows:

$$M_{ac}^t = \sigma(W_a \cdot \delta_a(\Phi_v(v^t))) \in \mathbb{R}^{C_a \times 1}, \quad (2)$$

with $\Phi_v(\cdot)$ aggregating video spatial features and $\delta_a(\cdot)$ aligning dimensions. The refined features are then obtained as $v_{cm}^t = v^t \odot M_{vc}^t$ and $a_{cm}^t = a^t \odot M_{ac}^t$, where \odot denotes channel-wise multiplication.

Spatial attention focuses on cross-modal positional importance distributions through modality-specific pooling:

$$M_{vs}^t = \sigma(\Psi_a(a^t)) \in \mathbb{R}^{1 \times (H \times W)}, \quad (3)$$

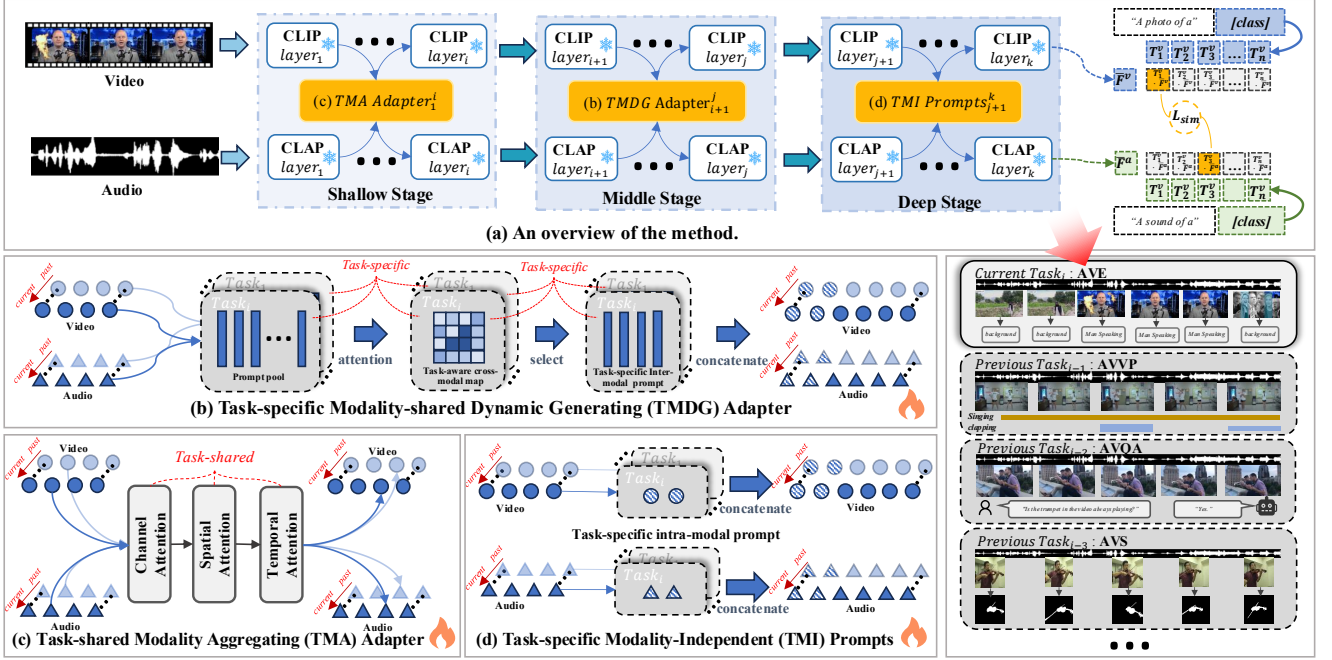


Figure 2. The Progressive Homeostatic and Plastic audio-visual prompt (PHP) framework consists of three stages for balancing knowledge preservation and transfer: (a) an overview of the three-stage architecture, (b) a task-specific modality-shared dynamic generating adapter for balancing anti-forgetting and multi-task transfer abilities, (c) a task-shared modality aggregating adapter in shallow stage for learning cross-task and cross-modal representations, and (d) task-specific modality-independent prompts in deep stage for preserving task-specific and modality-specific features.

$$M_{as}^t = \sigma(\Psi_v(v^t)) \in \mathbb{R}^{1 \times (L \times F)}, \quad (4)$$

where $\Psi_a(\cdot)$ and $\Psi_v(\cdot)$ implement squeeze-excitation operations to distill spatial dependencies.

Temporal synchronization is achieved through cascaded RNN layers to model sequential relationships. Given the temporal features a_{tmp}^t and v_{tmp}^t extracted via dense projection:

$$M_{vt}^t = \sigma(\Gamma_a(RNN(a_{tmp}^t))) \in \mathbb{R}^{1 \times (H \times W)}, \quad (5)$$

$$M_{at}^t = \sigma(\Gamma_v(RNN(v_{tmp}^t))) \in \mathbb{R}^{1 \times (H \times W)}, \quad (6)$$

where RNN is the recurrent neural network to explore the temporal information from video and audio, Γ_a and Γ_v map RNN hidden states to temporal attention scores. The final fused representations integrate the multi-perspective attention through learnable coefficients as formed by:

$$\tilde{V}^t = (\alpha \cdot M_{vc}^t \oplus \beta \cdot M_{vs}^t \oplus \gamma \cdot M_{vt}^t) \odot v^t, \quad (7)$$

$$\tilde{A}^t = (\alpha \cdot M_{ac}^t \oplus \beta \cdot M_{as}^t \oplus \gamma \cdot M_{at}^t) \odot a^t, \quad (8)$$

where \oplus indicates broadcast addition for dimensional compatibility. This consolidated fusion enables the model to learn generalized cross-modal patterns while preserving task-specific discriminability in shallow layers.

3.4. Task-specific Modality-shared Dynamic Generating Adapter

A large number of trainable shared parameters can bring considerable multi-task generalization capabilities to the

model, but at the same time, they may also introduce task interference and catastrophic forgetting issues between tasks with large domain gaps. Therefore, we propose the Task-specific Modality-shared Dynamic Generating (TMDG) adapter to balance the model's anti-forgetting capability with its multi-task generalization ability. Unlike the TMA adapter, we aim for TMA to learn a general audio-visual cross-modal representation that is applicable to most audio-visual tasks. In contrast, we designed the TMDG adapter to guide the model in refining deeper task-specific cross-modal representations for different audio-visual tasks. This enables the model to achieve excellent multi-task anti-forgetting capabilities as well as audio-video interaction capabilities for specific tasks.

The TMDG operates through a dual-phase process: (1) *prompt pool-based task concept mining* and (2) *dynamic instance-aware prompt generation*. Given a predefined prompt pool $\mathcal{P} = \{p_1, \dots, p_L\} \in \mathbb{R}^{L \times d}$, the visual feature $\mathcal{V} \in \mathbb{R}^{T \times D}$ and the audio feature $\mathcal{A} \in \mathbb{R}^{T \times D}$ undergo cross-modal fusion through concatenation with prompts, followed by self-attention operations to establish task-specific audio-visual semantic representations. This hierarchical integration process is formally defined as:

$$S_v = \text{AvgPool}(\text{SelfAttn}([\mathcal{V}; \mathcal{P}]]), \quad (9)$$

$$S_a = \text{AvgPool}(\text{SelfAttn}([\mathcal{A}; \mathcal{P}]]), \quad (10)$$

where $[\cdot; \cdot]$ denotes concatenation along the token dimension, $\text{SelfAttn}(\cdot)$ applies multi-head self-attention to

model cross-modal dependencies, and AvgPool consolidates temporal dimensions. Then the instance-wise global feature S_v and S_a are scaled and divided into n parts, guiding the prompt pool to select and generate prompts accordingly, where n is the length of the generated prompts. The formulation can be given as:

$$G_v = \delta_s(S_v) \cdot P \quad (11)$$

$$G_a = \delta_s(S_a) \cdot P \quad (12)$$

where $G_v \in \mathbb{R}^{n \times d}$ and $G_a \in \mathbb{R}^{n \times d}$ denote the generated prompts for visual and audio, respectively. δ_s is a projection layer to scale and divide the instance-wise theme into n parts for different specific prompts. Finally, the generated prompts are concatenated with the visual and audio features, and then feed into the CLIP and CLAP, respectively.

3.5. Task-specific Modality-independent Prompts

In the deep stage, in order to obtain audio-video features more specific to the current task and effectively mitigate the forgetting phenomenon, we introduce Task-specific Modality-Independent (TMI) prompts. While TMA learns shallow cross-modal patterns and TMDG generates task-aware representations, TMI separately preserves modality-critical details through hierarchical prompting. This module is based on task-specific prompts, providing the model with general task-level representations and relieving the issue caused by catastrophic forgetting. Additionally, for tasks similar to AVVP, it is necessary to make individual modal judgments between the audio and video modalities. The key details of a single modality still need to be preserved. Modal-independent prompts can ensure that the model refines key detail features on a single modality to guide the large model to output more task-discriminative and modality-characteristic information.

Given task index t and input features $\mathcal{V}^t \in \mathbb{R}^{T_v \times D}$ and $\mathcal{A}^t \in \mathbb{R}^{T_a \times D}$, TMI selects the corresponding prompt from different tasks due to the availability of tasks in audio-visual multi-task incremental learning. After selecting the visual and audio prompts, we concatenate them with visual and audio features to prompt the large model with a task-wise concept, the formulation is as follows:

$$PX_v = \text{concat}(P_v, V) \quad (13)$$

$$PX_a = \text{concat}(P_a, V) \quad (14)$$

where PX_v and PX_a denote the new features after being concatenated with the specific prompts P_v and P_a . Then prompt-guide features are fed into the large models to achieve a more discriminative clue for the specific task.

3.6. Optimizing Strategy

Given (v_i, a_i, t_i) as a piece of visual-audio-text pair indexed by i in the d -th task, the visual embedding F_i^v , the audio

embedding F_i^a and the corresponding text embedding T_i^v and T_i^a is encoded by:

$$F_i^v = MLP^v(\phi_v(v_i)) \quad F_i^a = MLP^a(\phi_a(a_i)) \quad (15)$$

$$T_i^v = MLP_t^v(\phi_t^v(t_i)) \quad F_i^a = MLP_t^a(\phi_t^a(t_i)) \quad (16)$$

where $MLPs$ are the 2-layer multilayer perception with ReLU for visual/audio/text respectively to project them into the same dimension. Then the model employs the contrastive constraint between the paired visual and text embeddings, followed by CLIP. Similar to CLIP, the paired audio and text embeddings conduct the contrastive constraints followed by CLAP, the formulations can be written as:

$$\mathcal{L}_v = \frac{1}{2N} \sum_{i=1}^N \left(\log \frac{\exp(F_i^v \cdot T_i^v / \tau_v)}{\sum_{j=1}^N \exp(F_i^v \cdot T_j^v / \tau_v)} + \log \frac{\exp(T_i^v \cdot F_i^v / \tau_v)}{\sum_{j=1}^N \exp(T_i^v \cdot F_j^v / \tau_v)} \right) \quad (17)$$

$$\mathcal{L}_a = \frac{1}{2N} \sum_{i=1}^N \left(\log \frac{\exp(F_i^a \cdot T_i^a / \tau_a)}{\sum_{j=1}^N \exp(F_i^a \cdot T_j^a / \tau_a)} + \log \frac{\exp(T_i^a \cdot F_i^a / \tau_a)}{\sum_{j=1}^N \exp(T_i^a \cdot F_j^a / \tau_a)} \right) \quad (18)$$

where τ_v and τ_a are learnable temperature parameters to adjust the loss. N represents the batch size, $\exp(\cdot)$ denote the exponential function.

4. Experiments

In this work, we simulate audio-visual multi-task incremental learning by treating multiple audio-visual tasks as a continuous data stream. We employ multiple different audio-visual understanding tasks, including audio-visual event localization (AVE), audio-visual video parsing (AVVP), audio-visual question answering (AVQA) and audio-visual segmentation (AVS). Detailed experimental settings can be found in the **supplementary material**.

4.1. Comparison Results

In this section, we conduct the comparison experiments between the proposed method PHP and the SOTA methods. The following methods can be divided into three groups: 1) Fine-tune-based method. This method addresses the newly arrived tasks by further fine-tuning the model based on the previous tasks. 2) Regularization-based method including EWC [24]. 3) Prompt-based methods including L2P [62], S-prompt [60], Dualprompt [61], PC [9], DCNet [59]. For fairness, the same pre-trained models (*i.e.* CLIP and CLAP) are used for all compared models as well as ours.

Comparison on anti-forgetting ability with the SOTA methods. Catastrophic forgetting is a key problem in incremental learning, and solving it is essential for models to

Table 1. Comparison on anti-forgetting ability with the SOTA methods. \uparrow indicates higher is better, \downarrow indicates lower is better. The best results are highlighted in bold.

Methods	AVE			AVVP			AVQA			$\bar{A}_{mean} \uparrow$	$\bar{F}_{mean} \downarrow$	$\bar{A}_{final} \uparrow$
	$A_{mean} \uparrow$	$A_{final} \uparrow$	$F_{mean} \downarrow$	$A_{mean} \uparrow$	$A_{final} \uparrow$	$F_{mean} \downarrow$	$A_{mean} \uparrow$	$A_{final} \uparrow$	$F_{mean} \downarrow$			
Fine-tune	29.61	12.74	22.37	48.52	38.30	7.17	53.66	53.49	0.35	43.93	9.96	34.84
EWC	8.52	2.38	7.71	22.55	1.08	30.97	56.73	56.70	0.00	29.26	12.89	20.05
L2P	52.05	34.25	17.78	41.43	33.23	7.75	59.77	59.80	-0.01	51.08	8.51	42.42
S-prompt	57.58	52.75	4.78	40.36	30.13	9.15	59.17	59.21	-0.04	52.37	4.63	47.36
Dualprompt	63.00	58.10	5.03	37.31	28.30	8.81	63.39	63.47	-0.08	54.57	4.59	49.95
PC	62.02	54.44	7.62	39.07	30.98	7.03	69.55	69.46	0.04	56.88	4.90	51.63
DCNet	30.43	12.75	23.29	48.75	39.17	6.52	53.34	53.86	0.16	44.17	9.99	35.26
Ours	62.03	55.00	6.72	45.25	40.67	2.22	69.29	68.56	1.01	58.85	3.32	54.74

Table 2. Comparison on multi-task transfer ability with the SOTA methods. A_{single} and A_{multi} represent the performance of single-task and multi-task training, respectively. The best results are highlighted in bold and Diff indicates the normalized improvement with quadratic baseline penalty. (Details can be seen in supplementary.)

Methods	Venue	AVE		AVVP		AVQA		\bar{A}_{single}	\bar{A}_{multi}	Diff
		$A_{single} \uparrow$	$A_{multi} \uparrow$	$A_{single} \uparrow$	$A_{multi} \uparrow$	$A_{single} \uparrow$	$A_{multi} \uparrow$			
Fine-tune	-	57.47	18.22	52.64	59.00	54.19	54.13	54.77	43.78	-58.16%
EWC	PNAS'17	17.79	18.00	63.01	62.67	56.70	54.64	45.83	45.10	-2.87%
L2P	CVPR'22	69.80	67.55	48.72	42.84	59.79	60.04	59.44	56.81	-16.46%
S-prompt	NeurIPS'22	62.31	54.39	48.42	42.84	59.13	54.57	56.62	50.60	-34.01%
Dualprompt	ECCV'22	68.15	67.48	45.92	46.19	63.32	60.04	59.13	57.90	-7.59%
PC	ACM MM'24	69.67	68.04	45.04	44.61	69.54	69.85	61.41	60.83	-3.94%
DCNet	ARXIV'25	59.33	19.06	52.20	57.60	54.18	53.97	55.24	43.54	-62.98%
Ours	-	70.45	72.52	47.80	48.60	68.84	69.30	62.36	63.47	+7.79%

Table 3. Ablation study on anti-forgetting ability.

Row	TMA adapter	TMDG adapter	TMI prompts	$\bar{A}_{mean} \uparrow$	$\bar{A}_{final} \uparrow$	$\bar{F}_{mean} \downarrow$
1				58.20	54.22	4.20
2	✓			58.23	55.07	3.34
3		✓		59.20	55.41	3.39
4			✓	59.70	55.84	3.78
5	✓	✓		59.54	56.01	3.21
6	✓		✓	58.87	55.20	3.76
7		✓	✓	59.28	45.51	3.90
8	✓	✓	✓	58.85	54.74	3.32

remember old information while learning new tasks. In this experiment, we demonstrate the anti-forgetting capability of our model by comparing it with the SOTA methods. Table 1 shows the comparison on three tasks, including AVE, AVVP and AVQA. The experiment is conducted on different incremental orders (the detailed results can be seen in the supplementary), and then we compute the mean accuracy and forget of different tasks. \bar{A}_{mean} , \bar{F}_{mean} and \bar{A}_{final} are computed as mean accuracy, mean forgetting scores and final accuracy by all tasks, respectively.

As shown in Table 1, our approach outperforms the other methods in terms of all metrics. Specifically, we notice that the mean accuracy is higher than that of other methods, which shows that our method performs better on audio-visual tasks. The mean forgetting score is 1.58% lower than the SOTA prompt-based incremental method, which demonstrates our model has a more significant ability to mitigate the forgetting issue resulting from the incremental process. The outstanding mean of the final accuracy also illustrates that our model can effectively maintain the initial

performance after training with two different tasks.

Comparison on multi-task transfer ability with the SOTA methods. The experiment primarily demonstrates the transfer ability of our model by comparing it with the state-of-the-art methods. As shown in Table 2, our method achieves the highest single-task performance (62.36%) and multi-task performance (63.47%) across all compared approaches. Most importantly, while all baseline methods exhibit negative transfer (ranging from -2.87% to -62.98%), our method is the only one showing positive transfer ability with a significant improvement of +7.79%. This indicates that our progressive prompting approach effectively leverages knowledge from previously learned tasks to benefit new tasks. Specifically, on the AVE task, our method surpasses others with both the highest single-task accuracy (70.45%) and a notable improvement after multi-task learning (72.52%). For AVVP and AVQA tasks, our approach consistently maintains strong performance, avoiding the performance degradation that affects competing methods. These results validate the effectiveness of our hierar-

Table 4. Ablation study on transfer ability.

Row	TMA adapter	TMDG adapter	TMI prompts	\bar{A}_{single}	\bar{A}_{multi}	Diff
1				62.62	61.76	-6.10%
2	✓			61.75	62.93	+8.05%
3		✓		62.20	62.14	-0.37%
4			✓	63.41	63.34	-0.48%
5	✓	✓		62.44	63.12	+4.77%
6	✓		✓	62.73	64.26	+7.99%
7		✓	✓	63.31	63.21	-0.71%
8	✓	✓	✓	62.36	63.47	+7.77%

chical design in balancing task-specific learning and cross-task knowledge transfer.

4.2. Ablation Studies

In this section, we conduct the ablation experiments to prove the effectiveness of each module or task order.

Ablation study on anti-forgetting ability. Table 3 presents the ablation results on anti-forgetting performance. The baseline (Row 1) shows moderate performance with mean forgetting of 4.20%. Each component makes unique contributions: TMI prompts achieve the highest average accuracy ($\bar{A}_{mean} = 59.70\%$) and final accuracy while the TMA+TMDG combination (Row 5) yields the lowest forgetting rate ($\bar{F}_{mean} = 3.21\%$) and highest final accuracy ($\bar{A}_{final} = 56.01\%$). This demonstrates how different components contribute to maintaining performance and mitigating catastrophic forgetting in audio-visual incremental learning.

Ablation study on transfer ability. Table 4 analyzes each component’s contribution to knowledge transfer. Without any components (Row 1), the model shows significant negative transfer (-6.10%). The TMA adapter alone (Row 2) achieves strong positive transfer (+8.05%), highlighting the importance of universal cross-modal representations. The TMA+TMI configuration (Row 6) and full model (Row 8) deliver similarly strong transfer capabilities (+7.99% and +7.77%). Interestingly, TMDG+TMI (Row 7) shows negative transfer (-0.71%), indicating that without TMA’s foundational representations, higher-level components cannot effectively share knowledge across tasks.

Ablation study on different component orders. Tables 5 and 6 present a comprehensive analysis of different com-

Table 5. Ablation study on different orders of TMA adapter, TMDG adapter, and TMI prompts.

Row	TMA adapter	TMDG adapter	TMI prompts	$A_{mean} \uparrow$	$A_{final} \uparrow$	$F_{mean} \downarrow$
1	D	M	S	47.29	41.14	7.29
2	M	D	S	48.85	43.32	5.42
3	D	S	M	48.32	44.17	5.89
4	M	S	D	49.12	42.73	7.41
5	S	D	M	47.82	43.08	5.70
6	S	M	D	58.85	54.74	3.32

Table 6. Ablation study on transfer ability with different orders of components.

Row	TMA adapter	TMDG adapter	TMI prompts	$A_{single} \uparrow$	$A_{multi} \uparrow$	Diff
1	D	M	S	55.72	55.43	-1.55%
2	M	D	S	54.17	55.38	+6.30%
3	D	S	M	55.95	57.08	+6.20%
4	M	S	D	57.55	56.60	-5.57%
5	S	D	M	54.47	54.98	+2.69%
6	S	M	D	62.36	63.47	+7.77%

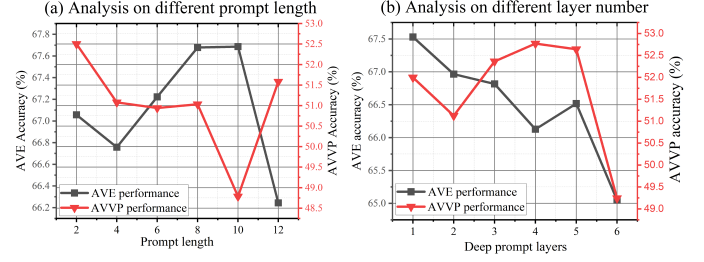


Figure 3. Ablation studies on key design parameters. (a) Impact of prompt length on model performance. (b) Effect of task-specific layer depth on AVE and AVVP performance.

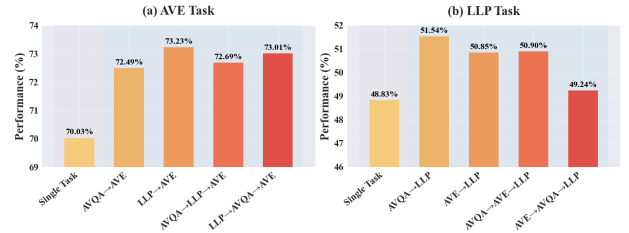


Figure 4. Performance analysis of multi-task training sequences. Comparison of different training orders on (a) AVE task and (b) LLP task performance.

ponent arrangements, where S indicates placement in shallow layers, M in middle layers, and D in deep layers. As shown in Table 5, the ”S-M-D” configuration (our proposed progressive arrangement) significantly outperforms alternative orderings with the highest mean accuracy (58.85%) and lowest forgetting rate (3.32%). Table 6 further demonstrates that this progressive ordering achieves optimal transfer capability with the highest single-task (62.36%) and multi-task (63.47%) performances. In contrast, configurations with ”D” or ”M” components in shallow layers exhibit higher forgetting rates and negative transfer effects. These results strongly validate our progressive design principle, where universal representations are learned at shallow layers, task-specific cross-modal features at middle layers, and fine-grained task-modality details at deeper layers.

Ablation study on deep prompts. **Ablation study on deep prompts.** We investigate how prompt length and number of injected layers affect model performance using the AVE→AVQA→AVVP sequence. We track AVE performance to evaluate forgetting resistance and AVVP performance to assess transfer capability. As shown in Fig. 3(a), increasing prompt length improves resistance to forgetting but reduces knowledge transfer efficiency, revealing a clear trade-off between memory retention and cross-task generalization. Fig. 3(b) demonstrates that increasing task-specific layers gradually degrades AVE performance, while AVVP performance first improves then sharply declines beyond the optimal configuration. This indicates that moderate task-specific parameterization helps capture relevant fea-

tures, but excessive parameters harm knowledge transferability across tasks.

Ablation study between single-task and multi-task.

Fig. 4 presents the performance analysis of different training sequences on AVE and LLP tasks. For AVE task (a), the model achieves 70.03% accuracy in single-task training, while all incremental sequences show improved performance, with LLP→AVE achieving the highest at 73.23%. For LLP task (b), AVQA→LLP sequence performs best at 51.54%, significantly outperforming the single-task baseline of 48.83%. The results demonstrate that appropriate task ordering in incremental learning can enhance model performance beyond single-task training.

Incremental learning on Four-Task Sequence. We further investigate our method on longer task sequences with four consecutive audio-visual tasks. As shown in Table 7, our approach shows remarkable stability across different task orderings. For the AVS→AVQA→AVVP→AVE sequence, the model maintains consistent performance on the initial task (55.51% final accuracy) while successfully learning subsequent tasks. Similarly, in the AVE→AVVP→AVS→AVQA order, our method preserves strong performance on earlier tasks while effectively transferring knowledge to new domains. These results validate that our progressive prompting strategy scales effectively to longer task sequences while maintaining a favorable bal-



Figure 5. Qualitative Results. We compare our method with baseline (without prompts) on AVE, AVVP, and AVQA. Our method demonstrates superior performance in maintaining accurate cross-modal understanding and temporal localization.

Table 7. Performance across different four-task incremental learning sequences.

Four-Task Incremental Learning								
Stage	AVS→AVQA→AVVP→AVE				AVE→AVVP→AVS→AVQA			
1	58.62				70.77			
2	54.25	69.36			60.17	48.00		
3	54.28	66.31	48.60		60.60	44.42	58.82	
4	55.51	66.61	31.48	69.88	59.58	50.90	53.19	69.80

ance between knowledge retention and transfer capability.

4.3. Quantitative Results

To provide an intuitive understanding of our method’s effectiveness, we visualize results across three audio-visual tasks in Fig 5. For the AVE task, our method accurately identifies ”Banjo” segments, while the baseline confuses it with ”Flute” and ”Accordion”, demonstrating our model’s superior cross-modal feature alignment. In AVVP, both approaches correctly detect motorcycle sounds, but our method achieves more precise temporal localization, validating the effectiveness of our task-specific adapter design. For AVQA, our approach correctly answers all questions about the musical instrument (ukulele), while the baseline misidentifies it as an acoustic guitar and incorrectly counts the number of instruments. These qualitative results not only demonstrate our model’s superior ability to maintain accurate cross-modal understanding but also highlight its effectiveness in preserving task-specific features through incremental learning. The consistent performance across diverse tasks further validates the robustness of our work.

5. Conclusion

In this paper, we present progressive homeostatic and plastic prompts for audio-visual multi-task incremental learning. Our method effectively addresses two key challenges: balancing task interference with knowledge sharing and maintaining modality specificity while promoting generality. Through a three-stage prompting strategy, PHP progressively refines audio-visual representations: the task-shared modality aggregating adapter enables cross-modal learning in shallow layers, the task-specific modality-shared dynamic generating adapter balances knowledge retention in middle layers, and the task-specific modality-independent prompts preserve task features in deep layers. Extensive experiments on three audio-visual tasks (AVE, AVVP, AVS and AVQA) demonstrate that our method significantly outperforms existing approaches in both preventing catastrophic forgetting and enabling effective knowledge transfer, validating the effectiveness of our work.

6. Acknowledgement

This work was supported by the ”Pioneer” and ”Leading Goose” R&D Program of Zhejiang Province(2023C01046,

2023C01038, 2024C01023), the National Nature Science Foundation of China (62322211, U21B2024, 62336008), Key Laboratory of Intelligent Processing Technology for Digital Music (Zhejiang Conservatory of Music), Ministry of Culture and Tourism (2023DMKLB004).

References

- [1] Rahaf Aljundi, Francesca Babiloni, Mohamed Elhoseiny, Marcus Rohrbach, and Tinne Tuytelaars. Memory aware synapses: Learning what (not) to forget. In *Proceedings of the European conference on computer vision (ECCV)*, pages 139–154, 2018. 1, 2
- [2] Hyojin Bahng, Ali Jahanian, Swami Sankaranarayanan, and Phillip Isola. Visual prompting: Modifying pixel space to adapt pre-trained models. *arXiv preprint arXiv:2203.17274*, 3(11-12):3, 2022. 3
- [3] Pietro Buzzega, Matteo Boschini, Angelo Porrello, Davide Abati, and Simone Calderara. Dark experience for general continual learning: a strong, simple baseline. *Advances in neural information processing systems*, 33:15920–15930, 2020. 1, 3
- [4] Hyuntak Cha, Jaeho Lee, and Jinwoo Shin. Co2l: Contrastive continual learning. In *Proceedings of the IEEE/CVF International conference on computer vision*, pages 9516–9525, 2021.
- [5] Arslan Chaudhry, Marcus Rohrbach, Mohamed Elhoseiny, Thalaiyasingam Ajanthan, Puneet K Dokania, Philip HS Torr, and Marcarcelo Ranzato. On tiny episodic memories in continual learning. *arXiv. Learning*, 6(7), 2019. 3
- [6] Haoran Chen, Zuxuan Wu, Xintong Han, Menglin Jia, and Yu-Gang Jiang. Promptfusion: Decoupling stability and plasticity for continual learning. *arXiv preprint arXiv:2303.07223*, 2023. 1, 3
- [7] Ke Chen, Xingjian Du, Bilei Zhu, Zejun Ma, Taylor Berg-Kirkpatrick, and Shlomo Dubnov. Hts-at: A hierarchical token-semantic audio transformer for sound classification and detection. In *ICASSP 2022-2022 IEEE International Conference on Acoustics, Speech and Signal Processing (ICASSP)*, pages 646–650. IEEE, 2022. 1
- [8] Yiming Cui, Liang Li, Jiehua Zhang, Chenggang Yan, Hongkui Wang, Shuai Wang, Heng Jin, and Li Wu. Stochastic context consistency reasoning for domain adaptive object detection. In *Proceedings of the 32nd ACM International Conference on Multimedia*, pages 1331–1340, 2024. 2
- [9] Yong Dai, Xiaopeng Hong, Yabin Wang, Zhiheng Ma, Dongmei Jiang, and Yaowei Wang. Prompt customization for continual learning. *arXiv preprint arXiv:2404.18060*, 2024. 2, 3, 5
- [10] Peihua Deng, Jiehua Zhang, Xichun Sheng, Chenggang Yan, Yaoqi Sun, Ying Fu, and Liang Li. Multi-granularity class prototype topology distillation for class-incremental source-free unsupervised domain adaptation. In *Proceedings of the Computer Vision and Pattern Recognition Conference*, pages 30566–30576, 2025. 3
- [11] Alexey Dosovitskiy, Lucas Beyer, Alexander Kolesnikov, Dirk Weissenborn, Xiaohua Zhai, Thomas Unterthiner, Mostafa Dehghani, Matthias Minderer, Georg Heigold, Sylvain Gelly, Jakob Uszkoreit, and Neil Houlsby. An image is worth 16x16 words: Transformers for image recognition at scale. *ICLR*, 2021. 1
- [12] Arthur Douillard, Alexandre Ramé, Guillaume Couairon, and Matthieu Cord. Dytox: Transformers for continual learning with dynamic token expansion. In *Proceedings of the IEEE/CVF Conference on Computer Vision and Pattern Recognition*, pages 9285–9295, 2022. 3
- [13] Haoyi Duan, Yan Xia, Zhou Mingze, Li Tang, Jieming Zhu, and Zhou Zhao. Cross-modal prompts: Adapting large pre-trained models for audio-visual downstream tasks. *Advances in Neural Information Processing Systems*, 36, 2024. 3
- [14] Sayna Ebrahimi, Franziska Meier, Roberto Calandra, Trevor Darrell, and Marcus Rohrbach. Adversarial continual learning. In *Computer Vision—ECCV 2020: 16th European Conference, Glasgow, UK, August 23–28, 2020, Proceedings, Part XI 16*, pages 386–402. Springer, 2020. 1, 3
- [15] Benjamin Elizalde, Soham Deshmukh, Mahmoud Al Ismail, and Huaming Wang. Clap learning audio concepts from natural language supervision. In *ICASSP 2023-2023 IEEE International Conference on Acoustics, Speech and Signal Processing (ICASSP)*, pages 1–5. IEEE, 2023. 3
- [16] Yingying Fan, Yu Wu, Bo Du, and Yutian Lin. Revisit weakly-supervised audio-visual video parsing from the language perspective. *Advances in Neural Information Processing Systems*, 36, 2024. 2
- [17] Shengyi Gao, Zhe Chen, Guo Chen, Wenhai Wang, and Tong Lu. Avsegformer: Audio-visual segmentation with transformer. In *Proceedings of the AAAI Conference on Artificial Intelligence*, pages 12155–12163, 2024. 2
- [18] YiHong Gong and GuoYin Wang. Preface: Brain-inspired ai research. *Science China Technological Sciences*, 67(8): 2281–2281, 2024. 3
- [19] Boyang Guo, Liang Li, Jiehua Zhang, Yaoqi Sun, Chenggang Yan, and Xichun Sheng. Prompt learning with knowledge regularization for pre-trained vision-language models. *IEEE Transactions on Multimedia*, 2025. Accepted for publication. 2
- [20] Qinghua Hu, Yucong Gao, and Bing Cao. Curiosity-driven class-incremental learning via adaptive sample selection. *IEEE Transactions on Circuits and Systems for Video Technology*, 32(12):8660–8673, 2022. 3
- [21] Tony Huang, Jack Chu, and Fangyun Wei. Unsupervised prompt learning for vision-language models. *arXiv preprint arXiv:2204.03649*, 2022. 2, 3
- [22] Dahuin Jung, Dongyoon Han, Jihwan Bang, and Hwanjun Song. Generating instance-level prompts for rehearsal-free continual learning. In *Proceedings of the IEEE/CVF International Conference on Computer Vision*, pages 11847–11857, 2023. 2, 3
- [23] Zixuan Ke, Bing Liu, and Xingchang Huang. Continual learning of a mixed sequence of similar and dissimilar tasks. *Advances in neural information processing systems*, 33:18493–18504, 2020. 2
- [24] James Kirkpatrick, Razvan Pascanu, Neil Rabinowitz, Joel Veness, Guillaume Desjardins, Andrei A Rusu, Kieran

- Milan, John Quan, Tiago Ramalho, Agnieszka Grabska-Barwinska, et al. Overcoming catastrophic forgetting in neural networks. *Proceedings of the national academy of sciences*, 114(13):3521–3526, 2017. 1, 2, 5
- [25] Mingrui Lao, Nan Pu, Yu Liu, Kai He, Erwin M Bakker, and Michael S Lew. Coca: Collaborative causal regularization for audio-visual question answering. In *Proceedings of the AAAI Conference on Artificial Intelligence*, pages 12995–13003, 2023. 2
- [26] Guangyao Li, Yake Wei, Yapeng Tian, Chenliang Xu, Ji-Rong Wen, and Di Hu. Learning to answer questions in dynamic audio-visual scenarios. In *Proceedings of the IEEE/CVF Conference on Computer Vision and Pattern Recognition*, pages 19108–19118, 2022. 1
- [27] Guangyao Li, Wenxuan Hou, and Di Hu. Progressive spatio-temporal perception for audio-visual question answering. In *Proceedings of the 31st ACM International Conference on Multimedia*, pages 7808–7816, 2023. 2
- [28] Xilai Li, Yingbo Zhou, Tianfu Wu, Richard Socher, and Caiming Xiong. Learn to grow: A continual structure learning framework for overcoming catastrophic forgetting. In *International conference on machine learning*, pages 3925–3934. PMLR, 2019. 2
- [29] Zhizhong Li and Derek Hoiem. Learning without forgetting. *IEEE transactions on pattern analysis and machine intelligence*, 40(12):2935–2947, 2017. 1, 2
- [30] Zeyi Li, Pan Wang, and Zixuan Wang. Flowganomaly: Flow-based anomaly network intrusion detection with adversarial learning. *Chinese Journal of Electronics*, 33(1):58–71, 2024. 2
- [31] Yan-Bo Lin, Yu-Jhe Li, and Yu-Chiang Frank Wang. Dual-modality seq2seq network for audio-visual event localization. In *ICASSP 2019-2019 IEEE International Conference on Acoustics, Speech and Signal Processing (ICASSP)*, pages 2002–2006. IEEE, 2019. 2
- [32] Yan-Bo Lin, Hung-Yu Tseng, Hsin-Ying Lee, Yen-Yu Lin, and Ming-Hsuan Yang. Exploring cross-video and cross-modality signals for weakly-supervised audio-visual video parsing. *Advances in Neural Information Processing Systems*, 34:11449–11461, 2021. 2
- [33] Jinxiang Liu, Yu Wang, Chen Ju, Chaofan Ma, Ya Zhang, and Weidi Xie. Annotation-free audio-visual segmentation. In *Proceedings of the IEEE/CVF Winter Conference on Applications of Computer Vision*, pages 5604–5614, 2024. 2
- [34] Xuejing Liu, Liang Li, Shuhui Wang, Zheng-Jun Zha, Zechao Li, Qi Tian, and Qingming Huang. Entity-enhanced adaptive reconstruction network for weakly supervised referring expression grounding. *IEEE Transactions on Pattern Analysis and Machine Intelligence*, 45(3):3003–3018, 2022. 2
- [35] XinCheng Lu, ZiQi Yuan, YiChi Zhang, HaiLin Ai, SiYuan Cheng, YiRan Ge, Fang Fang, and NiHong Chen. A comparison of statistical learning of naturalistic textures between dcnn and the human visual hierarchy. *Science China Technological Sciences*, 67(8):2310–2318, 2024. 3
- [36] XinCheng Lu, ZiQi Yuan, YiChi Zhang, HaiLin Ai, SiYuan Cheng, YiRan Ge, Fang Fang, and NiHong Chen. A comparison of statistical learning of naturalistic textures between dcnn and the human visual hierarchy. *Science China Technological Sciences*, 67(8):2310–2318, 2024. 3
- [37] Jie Ma, Min Hu, Pinghui Wang, Wangchun Sun, Lingyun Song, Hongbin Pei, Jun Liu, and Youtian Du. Look, listen, and answer: Overcoming biases for audio-visual question answering. *arXiv preprint arXiv:2404.12020*, 2024. 2
- [38] Arun Mallya and Svetlana Lazebnik. Packnet: Adding multiple tasks to a single network by iterative pruning. In *Proceedings of the IEEE conference on Computer Vision and Pattern Recognition*, pages 7765–7773, 2018. 2
- [39] Michael McCloskey and Neal J Cohen. Catastrophic interference in connectionist networks: The sequential learning problem. In *Psychology of learning and motivation*, pages 109–165. Elsevier, 1989. 2
- [40] Shentong Mo and Yapeng Tian. Multi-modal grouping network for weakly-supervised audio-visual video parsing. *Advances in Neural Information Processing Systems*, 35:34722–34733, 2022. 2
- [41] Yixin Ou, Yunzhi Yao, Ningyu Zhang, Hui Jin, Jiacheng Sun, Shumin Deng, Zhenguo Li, and Huajun Chen. How do llms acquire new knowledge? a knowledge circuits perspective on continual pre-training. *arXiv preprint arXiv:2502.11196*, 2025. 2
- [42] Jinxue Peng, Yong Wang, Jingfeng Xue, and Zhenyan Liu. Fast cross-platform binary code similarity detection framework based on cfgs taking advantage of nlp and inductive gnn. *Chinese Journal of Electronics*, 33(1):128–138, 2024. 2
- [43] Quang Pham, Chenghao Liu, and Steven Hoi. Dualnet: Continual learning, fast and slow. *Advances in Neural Information Processing Systems*, 34:16131–16144, 2021. 1, 3
- [44] Ameya Prabhu, Philip HS Torr, and Puneet K Dokania. Gdumb: A simple approach that questions our progress in continual learning. In *Computer Vision—ECCV 2020: 16th European Conference, Glasgow, UK, August 23–28, 2020, Proceedings, Part II 16*, pages 524–540. Springer, 2020. 1, 3
- [45] Alec Radford, Jong Wook Kim, Chris Hallacy, Aditya Ramesh, Gabriel Goh, Sandhini Agarwal, Girish Sastry, Amanda Askell, Pamela Mishkin, Jack Clark, et al. Learning transferable visual models from natural language supervision. In *International conference on machine learning*, pages 8748–8763. PMLR, 2021. 3
- [46] Jathushan Rajasegaran, Munawar Hayat, Salman H Khan, Fahad Shahbaz Khan, and Ling Shao. Random path selection for continual learning. *Advances in neural information processing systems*, 32, 2019. 2
- [47] Andrei A Rusu, Neil C Rabinowitz, Guillaume Desjardins, Hubert Soyer, James Kirkpatrick, Koray Kavukcuoglu, Razvan Pascanu, and Raia Hadsell. Progressive neural networks. *arXiv preprint arXiv:1606.04671*, 2016. 2
- [48] Joan Serra, Didac Suris, Marius Miron, and Alexandros Karatzoglou. Overcoming catastrophic forgetting with hard attention to the task. In *International conference on machine learning*, pages 4548–4557. PMLR, 2018. 2
- [49] Chao Shang, Hongliang Li, Fanman Meng, Qingbo Wu, Heqian Qiu, and Lanxiao Wang. Incrementer: Transformer

- for class-incremental semantic segmentation with knowledge distillation focusing on old class. In *Proceedings of the IEEE/CVF Conference on Computer Vision and Pattern Recognition*, pages 7214–7224, 2023. 2
- [50] Reza Shokri and Vitaly Shmatikov. Privacy-preserving deep learning. In *Proceedings of the 22nd ACM SIGSAC conference on computer and communications security*, pages 1310–1321, 2015. 3
- [51] James Seale Smith, Leonid Karlinsky, Vyshnavi Gutta, Paola Cascante-Bonilla, Donghyun Kim, Assaf Arbelle, Rameswar Panda, Rogerio Feris, and Zsolt Kira. Coda-prompt: Continual decomposed attention-based prompting for rehearsal-free continual learning. In *Proceedings of the IEEE/CVF Conference on Computer Vision and Pattern Recognition*, pages 11909–11919, 2023. 2, 3
- [52] Yapeng Tian, Jing Shi, Bochen Li, Zhiyao Duan, and Chenliang Xu. Audio-visual event localization in unconstrained videos. In *Proceedings of the European conference on computer vision (ECCV)*, pages 247–263, 2018. 2, 1
- [53] Yapeng Tian, Jing Shi, Bochen Li, Zhiyao Duan, and Chenliang Xu. Audio-visual event localization in the wild. In *IEEE Computer Society Conference on Computer Vision and Pattern Recognition workshops*, 2019. 2
- [54] Yapeng Tian, Dingzeyu Li, and Chenliang Xu. Unified multisensory perception: Weakly-supervised audio-visual video parsing. In *Computer Vision–ECCV 2020: 16th European Conference, Glasgow, UK, August 23–28, 2020, Proceedings, Part III 16*, pages 436–454. Springer, 2020. 2, 1
- [55] Ye Tian, Ying Fu, and Jun Zhang. Transformer-based under-sampled single-pixel imaging. *Chinese Journal of Electronics*, 32(5):1151–1159, 2023. 2
- [56] Yunbin Tu, Liang Li, Li Su, Zheng-Jun Zha, and Qingming Huang. Smart: Syntax-calibrated multi-aspect relation transformer for change captioning. *IEEE Transactions on Pattern Analysis and Machine Intelligence*, 46(7):4926–4943, 2024. 2
- [57] GuoYin Wang, HuaNan Bao, Qun Liu, TianGang Zhou, Si Wu, TieJun Huang, ZhaoFei Yu, CeWu Lu, YiHong Gong, ZhaoXiang Zhang, et al. Brain-inspired artificial intelligence research: A review. *Science China Technological Sciences*, 67(8):2282–2296, 2024. 3
- [58] Hao Wang, Zheng-Jun Zha, Liang Li, Xuejin Chen, and Jiebo Luo. Semantic and relation modulation for audio-visual event localization. *IEEE Transactions on Pattern Analysis and Machine Intelligence*, 45(6):7711–7725, 2022. 2
- [59] Tianqi Wang, Jingcai Guo, Depeng Li, and Zhi Chen. On the discrimination and consistency for exemplar-free class incremental learning. *arXiv preprint arXiv:2501.15454*, 2025. 5
- [60] Yabin Wang, Zhiwu Huang, and Xiaopeng Hong. S-prompts learning with pre-trained transformers: An occam’s razor for domain incremental learning. *Advances in Neural Information Processing Systems*, 35:5682–5695, 2022. 2, 3, 5
- [61] Zifeng Wang, Zizhao Zhang, Sayna Ebrahimi, Ruoxi Sun, Han Zhang, Chen-Yu Lee, Xiaoqi Ren, Guolong Su, Vincent Perot, Jennifer Dy, et al. Dualprompt: Complementary prompting for rehearsal-free continual learning. In *European Conference on Computer Vision*, pages 631–648. Springer, 2022. 3, 5
- [62] Zifeng Wang, Zizhao Zhang, Chen-Yu Lee, Han Zhang, Ruoxi Sun, Xiaoqi Ren, Guolong Su, Vincent Perot, Jennifer Dy, and Tomas Pfister. Learning to prompt for continual learning. In *Proceedings of the IEEE/CVF conference on computer vision and pattern recognition*, pages 139–149, 2022. 2, 3, 5
- [63] Yu Wu and Yi Yang. Exploring heterogeneous clues for weakly-supervised audio-visual video parsing. In *Proceedings of the IEEE/CVF Conference on Computer Vision and Pattern Recognition*, pages 1326–1335, 2021. 2
- [64] Yue Wu, Yinpeng Chen, Lijuan Wang, Yuancheng Ye, Zicheng Liu, Yandong Guo, and Yun Fu. Large scale incremental learning. In *Proceedings of the IEEE/CVF conference on computer vision and pattern recognition*, pages 374–382, 2019. 1, 3
- [65] Yu Wu, Linchao Zhu, Yan Yan, and Yi Yang. Dual attention matching for audio-visual event localization. In *Proceedings of the IEEE/CVF international conference on computer vision*, pages 6292–6300, 2019. 2
- [66] Chenggang Yan, Biao Gong, Yuxuan Wei, and Yue Gao. Deep multi-view enhancement hashing for image retrieval. *IEEE Transactions on Pattern Analysis and Machine Intelligence*, 43(4):1445–1451, 2020. 2
- [67] Chenggang Yan, Zhisheng Li, Yongbing Zhang, Yutao Liu, Xiangyang Ji, and Yongdong Zhang. Depth image denoising using nuclear norm and learning graph model. *ACM Transactions on Multimedia Computing, Communications, and Applications (TOMM)*, 16(4):1–17, 2020. 2
- [68] Chenggang Yan, Yiming Hao, Liang Li, Jian Yin, Anan Liu, Zhendong Mao, Zhenyu Chen, and Xingyu Gao. Task-adaptive attention for image captioning. *IEEE Transactions on Circuits and Systems for Video technology*, 32(1):43–51, 2021. 2
- [69] Chenggang Yan, Tong Teng, Yutao Liu, Yongbing Zhang, Haoqian Wang, and Xiangyang Ji. Precise no-reference image quality evaluation based on distortion identification. *ACM Transactions on Multimedia Computing, Communications, and Applications (TOMM)*, 17(3s):1–21, 2021. 2
- [70] Chenggang Yan, Lixuan Meng, Liang Li, Jiehua Zhang, Zhan Wang, Jian Yin, Jiyong Zhang, Yaoqi Sun, and Bolun Zheng. Age-invariant face recognition by multi-feature fusion and decomposition with self-attention. *ACM Transactions on Multimedia Computing, Communications, and Applications (TOMM)*, 18(1s):1–18, 2022.
- [71] Chenggang Yan, Yaoqi Sun, Hao Zhong, Chenwei Zhu, Zunjie Zhu, Bolun Zheng, and Xiaofei Zhou. Review of omni-media content quality evaluation. *J. Signal Process.*, 38(6):1111–1143, 2022. 2
- [72] Shipeng Yan, Jiangwei Xie, and Xuming He. Der: Dynamically expandable representation for class incremental learning. In *Proceedings of the IEEE/CVF conference on computer vision and pattern recognition*, pages 3014–3023, 2021. 2
- [73] Zhiwen Yang, Liang Li, Jiehua Zhang, Tingyu Wang, Yaoqi Sun, and Chenggang Yan. Domain shared and specific

- prompt learning for incremental monocular depth estimation. In *Proceedings of the 32nd ACM International Conference on Multimedia*, pages 8306–8315, 2024. [3](#)
- [74] Zhaoda Ye, Xiangteng He, and Yuxin Peng. Unsupervised cross-media hashing learning via knowledge graph. *Chinese Journal of Electronics*, 31(6):1081–1091, 2022. [2](#)
- [75] Zhaoda Ye, Xiangteng He, and Yuxin Peng. Unsupervised cross-media hashing learning via knowledge graph. *Chinese Journal of Electronics*, 31(6):1081–1091, 2022. [2](#)
- [76] Jaehong Yoon, Eunho Yang, Jeongtae Lee, and Sung Ju Hwang. Lifelong learning with dynamically expandable networks. *arXiv preprint arXiv:1708.01547*, 2017. [2](#)
- [77] Da Yu, Mingyi Zhang, Mantian Li, Fusheng Zha, Junge Zhang, Lining Sun, and Kaiqi Huang. Contrastive correlation preserving replay for online continual learning. *IEEE Transactions on Circuits and Systems for Video Technology*, 34(1):124–139, 2023. [3](#)
- [78] Friedemann Zenke, Ben Poole, and Surya Ganguli. Continual learning through synaptic intelligence. In *International conference on machine learning*, pages 3987–3995. PMLR, 2017. [1](#), [2](#)
- [79] Beichen Zhang, Liang Li, Shuhui Wang, Shaofei Cai, Zheng-Jun Zha, Qi Tian, and Qingming Huang. Inductive state-relabeling adversarial active learning with heuristic clique rescaling. *IEEE Transactions on Pattern Analysis and Machine Intelligence*, 2024. [2](#)
- [80] Tao Zhang, Ying Fu, and Jun Zhang. Deep guided attention network for joint denoising and demosaicing in real image. *Chinese Journal of Electronics*, 33(1):303–312, 2024.
- [81] Tao Zhang, Ying Fu, and Jun Zhang. Deep guided attention network for joint denoising and demosaicing in real image. *Chinese Journal of Electronics*, 33(1):303–312, 2024. [2](#)
- [82] Zhao Zhang, Yan Zhang, Mingliang Xu, Li Zhang, Yi Yang, and Shuicheng Yan. A survey on concept factorization: From shallow to deep representation learning. *Information Processing & Management*, 58(3):102534, 2021. [3](#)
- [83] Zhedong Zhang, Liang Li, Gaoxiang Cong, Haibing Yin, Yuhao Gao, Chenggang Yan, Anton van den Hengel, and Yuankai Qi. From speaker to dubber: movie dubbing with prosody and duration consistency learning. In *Proceedings of the 32nd ACM International Conference on Multimedia*, pages 7523–7532, 2024. [2](#)
- [84] Zhedong Zhang, Liang Li, Chenggang Yan, Chunshan Liu, Anton van den Hengel, and Yuankai Qi. Prosody-enhanced acoustic pre-training and acoustic-disentangled prosody adapting for movie dubbing. In *Proceedings of the Computer Vision and Pattern Recognition Conference*, pages 172–182, 2025.
- [85] Zhiqian Zhao, Liang Li, Jiehua Zhang, Yaoqi Sun, Xichun Sheng, Haibing Yin, and Shaowei Jiang. Heterogeneous prompt-guided entity inferring and distilling for scene-text aware cross-modal retrieval. In *Proceedings of the AAAI Conference on Artificial Intelligence*, pages 10537–10545, 2025. [2](#)
- [86] Jinkai Zheng, Xinchun Liu, Wu Liu, Lingxiao He, Chenggang Yan, and Tao Mei. Gait recognition in the wild with dense 3d representations and a benchmark. In *Proceedings of the IEEE/CVF conference on computer vision and pattern recognition*, pages 20228–20237, 2022. [2](#)
- [87] Jinxing Zhou, Jianyuan Wang, Jiayi Zhang, Weixuan Sun, Jing Zhang, Stan Birchfield, Dan Guo, Lingpeng Kong, Meng Wang, and Yiran Zhong. Audio–visual segmentation. In *European Conference on Computer Vision*, pages 386–403. Springer, 2022. [2](#), [1](#)

Progressive Homeostatic and Plastic Prompt Tuning for Audio-Visual Multi-Task Incremental Learning

Supplementary Material

A. Tasks and Datasets

In this work, we simulate audio-visual multi-task incremental learning by treating multiple audio-visual tasks as a continuous data stream. We employ multiple different audio-visual understanding tasks, including audio-visual event localization, audio-visual video parsing, audio-visual question answering and audio-visual segmentation.

Audio-Visual Event localization (AVE) [52] is concerned with identifying events within a video that are simultaneously visible and audible across various temporal intervals. We conduct an assessment of the AVE dataset, which includes 4,143 videos across 28 event categories and one background category. These 10-second videos depict diverse scenarios like musical performances.

Audio-Visual Video Parsing (AVVP) [54] aims to parse a video into temporal event sequences and categorize them as auditory, visual, or concurrently audio-visual. We perform experiments on the *Look, Listen, and Parse* (LLP) dataset, which consists of 11,849 10-second video clips across 25 real-life categories. We utilize 10,000 clips with weak annotations for training, and 1,849 clips with detailed annotations for testing and verification.

Audio-Visual Question Answering (AVQA) [26] is to answer questions by leveraging the correlations between visual objects and auditory cues. Experiments are conducted on the *MUSIC-AVQA* dataset, which features over 45,000 Q&A pairs in 9,288 videos totaling 150+ hours.

Audio-Visual Segmentation (AVS) [87] employs the Single Sound Source (S4) subset of AVSBench, comprising 4,932 videos (5 seconds each) with single sound-emitting objects. Each video aligns five 1-second audio clips and image frames, spanning 23 categories (e.g. human voice, instruments), and provides pixel-level annotations.

B. Experimental Setup

Metrics. In this work, we generally use accuracy to represent the performance of our model on three different tasks, which is divided into five metrics: A_{mean} , A_{final} , F_{mean} , A_{single} , and A_{multi} . A_{mean} represents the average accuracy of the task over three incremental settlements. A_{final} indicates the accuracy of the initial task after the incremental process. F_{mean} denotes the average forgetting rate of the initial task after the incremental process. A_{single} expresses the performance when the task is trained individually. A_{multi} is the accuracy of the final task after training on multiple tasks. With these five indicators, our aim is to ef-

fectively demonstrate: 1) The performance of the model on a particular task. 2) The degree of forgetting of the model during the multi-task incremental process. 3) The beneficial extent of previous tasks to subsequent tasks during the multi-task incremental process.

Implements details. Our model builds upon the pre-trained CLIP and CLAP architectures as its backbone for handling three audio-visual downstream tasks. Specifically, we utilize a frozen CLIP-trained ViT [11] for visual encoding and a frozen CLAP-trained HTS-AT [7] for audio encoding, leveraging their pre-trained parameters for robust multi-modal feature extraction. The prompts and adapters are strategically injected into both ViT and HTS-AT layers to facilitate audio-visual cross-modal correspondence while preserving knowledge from previous tasks. During training, we set the batch size to 3 and train each task for 10 epochs to ensure convergence. For the optimization process, we employ the Adam optimizer with a learning rate of $3e-4$ and a weight decay of $2e-4$. The learning rate is scheduled with a cosine decay strategy. We conduct all experiments on a single NVIDIA 3090 GPU with 24GB memory.

C. Normalized Penalty-aware Difference

To better evaluate the improvement of different methods in multi-task learning scenarios, we propose a novel evaluation metric called normalized penalty-aware difference (*Diff*). This metric is designed to address two key challenges in performance evaluation: (1) the difficulty of achieving improvements upon higher baseline performance, and (2) the unfair advantage of methods with lower baseline performance showing larger absolute improvements.

The metric is defined by incorporating both normalized improvement and baseline performance through a quadratic penalty term:

$$Diff = \frac{A_{multi} - A_{single}}{100 - A_{single}} \times \left(1 + \frac{A_{single}}{100}\right)^2 \times 100\% \quad (19)$$

where A_{multi} and A_{single} represent the performance of multi-task and single-task training respectively. The metric consists of three key components. First, the normalized improvement term $\frac{A_{multi} - A_{single}}{100 - A_{single}}$ considers the relative improvement potential by normalizing the performance gain against the remaining improvement headroom. Second, the quadratic baseline penalty $\left(1 + \frac{A_{single}}{100}\right)^2$ introduces a penalty that grows quadratically with the baseline

performance, reflecting the increasing difficulty of achieving improvements as the baseline performance gets higher. Finally, the multiplication by 100% converts the score into a percentage form for better interpretability.

To handle boundary cases where baseline performance approaches 100%, we introduce a small positive number ϵ (e.g., 0.001) to prevent division by zero:

$$Diff = \frac{A_{multi} - A_{single}}{\max(100 - A_{single}, \epsilon)} \times (1 + \frac{A_{single}}{100})^2 \times 100\% \quad (20)$$

In Table 2 in the main text, our metric provides a more nuanced evaluation of different methods’ capabilities. For example, while Fine-tune shows significant performance degradation on AVE (from 57.47% to 18.22%) but improvement on AVVP (from 52.64% to 59.00%), its overall Diff score of -58.16% indicates severe negative transfer. By comparison, EWC (-2.87%) and PC (-3.94%) demonstrate more stable performance but still fail to achieve positive knowledge transfer. Notably, despite PC achieving high performance on AVQA (69.85%), its overall transfer capability remains negative. In contrast, our method is the only approach showing positive knowledge transfer (+7.79%), with particularly strong performance on AVE (improving from 70.45% to 72.52%). These results clearly demonstrate that our progressive prompting approach effectively leverages knowledge from previously learned tasks to enhance performance on new tasks while maintaining robustness across both cross-task and cross-modal scenarios.

D. More Detailed Experiments of Comparison Methods

Here we provide more detailed experimental results to demonstrate the performance of different methods under various task orders. We evaluate six methods (Fine-tune, EWC, L2P, S-prompt, Dualprompt, and PC) across six different task ordering scenarios to track their performance through three stages of incremental learning. These comprehensive results allow us to analyze both the forgetting resistance and knowledge transfer capabilities of each method in detail.

Tab.8-Tab.13 present the complete performance metrics for each method. The progression of performance scores reveals distinct patterns in how different approaches handle catastrophic forgetting and knowledge transfer. When examining the performance trajectory, we observe that traditional methods like fine-tuning exhibit severe forgetting, with performance often deteriorating dramatically as new tasks are learned. For instance, in the AVE→AVVP→AVQA sequence, fine-tuning’s performance on AVE drops from 56.77% to 19.48% after learning AVVP, and further declines to 17.79% after learn-

ing AVQA, demonstrating significant knowledge erosion of the initial task. In contrast, the PC method demonstrates greater resilience to catastrophic forgetting. In the same AVE→AVVP→AVQA sequence, PC maintains the performance on AVE at 54.50% after learning all three tasks, compared to the original 69.90%. However, PC is not immune to forgetting, as evidenced in the AVVP→AVQA→AVE sequence where the performance on AVVP drops from 45.66% to 22.90% after learning all tasks. Notably, the task order significantly impacts performance retention, with certain sequences like AVQA→AVVP→AVE allowing PC to maintain relatively stable performance on the first task (69.44% from an initial 69.72%).

Table 14- 26 provide an extensive analysis of different component configurations and ordering strategies across various task sequences. Table 18 shows the detailed performance of the model without TMA-TMDG-TMI components under different task orders. Table 16- 18 demonstrate the performance of models with TMDG-TMI components, TMA-TMI components, and TMA-TMDG components removed, respectively. Table 19- 21 focus on ablation studies of individual components. Removing TMI (Table 19) affects task-specific representation refinement, while removing TMDG (Table 20) impairs cross-modal integration capabilities. Table 21 shows that without TMA, the model struggles to establish foundational audio-visual correspondences, particularly affecting performance on earlier tasks in the sequence. Table 22- 26 examine different ordering arrangements of our components across network depths: D-M-S (Table 22), M-D-S (Table 23), D-S-M (Table 24), M-S-D (Table 25), and S-D-M (Table 26) configurations, where D represents deep layers, M represents middle layers, and S represents shallow layers. The results consistently demonstrate that our proposed progressive S-M-D ordering (shallow-middle-deep) achieves optimal performance across different metrics and task sequences. This validates our key design principle: universal representations should be learned at shallow layers, task-specific cross-modal features at middle layers, and fine-grained task-modality details at deeper layers. These comprehensive results strongly support our architectural design choices and demonstrate the effectiveness of our progressive prompting strategy for audio-visual multi-task incremental learning.

Table 8. Performance analysis of fine-tuning under different task orders. Each column within an order shows the performance of tasks as they are incrementally learned.

fine-tune									
Stage	AVE→AVVP→AVQA			AVE→AVQA→AVVP			AVVP→AVE→AVQA		
1	56.77			58.16			51.95		
2	19.48	50.16		17.77	54.27		46.21	36.79	
3	17.79	63.01	54.18	7.69	53.02	59.71	63.01	17.79	54.08
Stage	AVVP→AVQA→AVE			AVQA→AVE→AVVP			AVQA→AVVP→AVE		
1	53.33			54.16			54.22		
2	63.01	54.21		54.24	18.11		54.00	58.70	
3	13.58	53.16	18.21	52.50	8.98	58.28	54.47	10.05	18.23

Table 9. Performance analysis of EWC under different task orders. Each column within an order shows the performance of tasks as they are incrementally learned. The first task’s performance is tracked across all stages to evaluate forgetting resistance, while the final task’s performance demonstrates transfer capability.

EWC									
Stage	AVE→AVVP→AVQA			AVE→AVQA→AVVP			AVVP→AVE→AVQA		
1	17.79			17.79			63.01		
2	9.68	63.01		1.07	54.97		5.51	17.79	
3	1.57	0.92	54.51	3.18	54.95	63.01	0.69	3.93	54.76
Stage	AVVP→AVQA→AVE			AVQA→AVE→AVVP			AVQA→AVVP→AVE		
1	63.01			54.44			58.95		
2	1.61	52.13		54.45	17.79		59.12	62.74	
3	1.47	52.51	17.74	54.30	4.55	62.32	59.10	62.55	18.26

Table 10. Performance analysis of L2P under different task orders. Each column within an order shows the performance of tasks as they are incrementally learned.

L2P									
Stage	AVE→AVVP→AVQA			AVE→AVQA→AVVP			AVVP→AVE→AVQA		
1	70.32			69.28			48.69		
2	34.83	48.32		69.35	60.03		35.47	65.45	
3	34.73	48.32	60.20	33.76	60.14	47.22	39.74	65.70	59.87
Stage	AVVP→AVQA→AVE			AVQA→AVE→AVVP			AVQA→AVVP→AVE		
1	48.74			59.30			60.28		
2	49.20	60.02		59.22	68.11		60.20	49.33	
3	26.71	59.99	68.41	59.31	68.21	42.72	60.28	38.64	66.69

Table 11. Performance analysis of S-prompt under different task orders. Each column within an order shows the performance of tasks as they are incrementally learned.

S-prompt									
Stage	AVE→AVVP→AVQA			AVE→AVQA→AVVP			AVVP→AVE→AVQA		
1	60.95			63.66			45.66		
2	51.27	42.50		64.08	58.75		34.10	48.71	
3	51.09	42.31	59.85	54.40	58.76	42.96	31.99	17.74	49.29
Stage	AVVP→AVQA→AVE			AVQA→AVE→AVVP			AVQA→AVVP→AVE		
1	51.17			59.30			58.95		
2	50.94	58.04		59.22	59.75		59.12	52.64	
3	28.27	58.08	54.25	59.31	51.94	42.72	59.10	43.32	54.53

Table 12. Performance analysis of Dualprompt under different task orders. Each column within an order shows the performance of tasks as they are incrementally learned.

Dualprompt									
Stage	AVE→AVVP→AVQA			AVE→AVQA→AVVP			AVVP→AVE→AVQA		
1	68.21			68.08			46.17		
2	58.26	45.85		67.26	64.69		29.14	68.46	
3	56.84	42.59	64.57	59.35	64.82	46.03	31.07	67.24	63.77
Stage	AVVP→AVQA→AVE			AVQA→AVE→AVVP			AVQA→AVVP→AVE		
1	45.66			63.48			63.15		
2	46.31	64.06		63.54	68.28		63.19	44.75	
3	25.52	64.06	67.91	63.75	54.35	46.35	63.19	34.97	67.04

Table 13. Performance analysis of PC under different task orders. Each column within an order shows the performance of tasks as they are incrementally learned.

PC									
Stage	AVE→AVVP→AVQA			AVE→AVQA→AVVP			AVVP→AVE→AVQA		
1	69.90			69.43			44.42		
2	55.50	45.89		68.38	69.24		36.90	66.57	
3	54.50	45.53	69.86	54.38	69.04	44.56	39.06	66.97	69.84
Stage	AVVP→AVQA→AVE			AVQA→AVE→AVVP			AVQA→AVVP→AVE		
1	45.66			69.35			69.72		
2	45.48	69.67		69.51	71.00		69.78	44.47	
3	22.90	69.62	68.86	69.47	56.27	44.65	69.44	30.61	67.21

Table 14. Performance analysis of DCNet under different task orders. Each column within an order shows the performance of tasks as they are incrementally learned.

DCNet									
Stage	AVE→AVVP→AVQA			AVE→AVQA→AVVP			AVVP→AVE→AVQA		
1	58.13			60.52			54.34		
2	20.62	48.83		17.79	54.25		46.73	38.06	
3	17.79	63.01	53.93	7.71	53.57	59.48	63.01	17.79	54.01
Stage	AVVP→AVQA→AVE			AVQA→AVE→AVVP			AVQA→AVVP→AVE		
1	50.07			54.23			54.13		
2	63.01	54.37		54.47	17.71		53.14	59.57	
3	15.33	50.38	18.28	54.20	5.92	55.71	53.52	7.71	19.83

Table 15. Ablation study: Detailed Performance of model without TMA-TMDG-TMI components under different task orders. Each column within an order shows the performance of tasks as they are incrementally learned.

w/o TMA-TMDG-TMI									
Stage	AVE→AVVP→AVQA			AVE→AVQA→AVVP			AVVP→AVE→AVQA		
1	70.67			70.87			48.14		
2	57.46	45.80		70.62	69.39		32.35	69.03	
3	58.96	45.76	69.82	57.56	69.61	46.49	34.33	69.25	70.17
Stage	AVVP→AVQA→AVE			AVQA→AVE→AVVP			AVQA→AVVP→AVE		
1	46.90			69.28			69.85		
2	47.04	69.94		69.60	69.78		69.48	47.64	
3	35.34	69.98	68.06	69.36	57.11	45.20	69.76	30.29	70.80

Table 16. Ablation study: Detailed Performance without TMDG-TMI components under different task orders.

w/o TMDG-TMI									
Stage	AVE→AVVP→AVQA			AVE→AVQA→AVVP			AVVP→AVE→AVQA		
1	68.91			69.45			45.53		
2	60.25	46.49		68.88	70.06		29.88	69.70	
3	62.79	51.95	70.17	59.65	69.72	48.55	35.57	63.48	70.27
Stage	AVVP→AVQA→AVE			AVQA→AVE→AVVP			AVQA→AVVP→AVE		
1	46.81			69.72			70.08		
2	49.34	70.71		69.27	71.49		69.53	48.97	
3	34.19	70.55	70.99	69.10	59.65	46.77	69.10	34.37	70.82

Table 17. Ablation study: Detailed Performance without TMA-TMI components under different task orders.

w/o TMA-TMI									
Stage	AVE→AVVP→AVQA			AVE→AVQA→AVVP			AVVP→AVE→AVQA		
1	70.03			71.19			46.95		
2	60.32	47.45		70.97	69.21		43.97	70.20	
3	61.77	47.13	70.07	59.15	69.30	47.32	39.70	69.88	69.49
Stage	AVVP→AVQA→AVE			AVQA→AVE→AVVP			AVQA→AVVP→AVE		
1	45.76			69.69			69.57		
2	45.53	69.47		69.36	69.13		69.73	48.28	
3	32.58	69.65	69.58	69.65	59.58	46.58	69.64	30.70	69.83

Table 18. Ablation study: Detailed performance without TMA-TMDG components under different task orders.

w/o TMA-TMDG									
Stage	AVE→AVVP→AVQA			AVE→AVQA→AVVP			AVVP→AVE→AVQA		
1	71.79			70.65			50.12		
2	62.31	49.01		70.57	69.55		39.01	71.42	
3	63.06	48.55	68.76	55.30	69.69	49.29	41.53	71.12	69.20
Stage	AVVP→AVQA→AVE			AVQA→AVE→AVVP			AVQA→AVVP→AVE		
1	48.88			69.95			69.08		
2	48.60	68.99		69.53	72.26		69.15	50.02	
3	34.65	68.90	71.37	69.69	62.36	48.23	70.81	36.99	73.21

Table 19. Ablation study: Detailed Performance without TMI component under different task orders.

w/o TMI									
Stage	AVE→AVVP→AVQA			AVE→AVQA→AVVP			AVVP→AVE→AVQA		
1	69.65			68.09			48.88		
2	58.16	47.50		68.33	69.68		45.07	71.37	
3	59.78	48.92	70.47	57.81	69.54	48.80	45.98	66.34	70.09
Stage	AVVP→AVQA→AVE			AVQA→AVE→AVVP			AVQA→AVVP→AVE		
1	47.87			70.10			70.05		
2	50.12	70.02		69.44	71.29		69.81	50.21	
3	33.73	69.92	71.22	69.55	57.44	47.18	69.23	36.90	70.95

Table 20. Ablation study: Detailed Performance without TMDG component under different task orders.

w/o TMDG									
Stage	AVE→AVVP→AVQA			AVE→AVQA→AVVP			AVVP→AVE→AVQA		
1	69.25			69.85			49.52		
2	58.38	47.73		68.33	70.09		40.71	70.52	
3	58.33	49.24	70.94	56.19	69.93	50.53	42.59	63.61	70.68
Stage	AVVP→AVQA→AVE			AVQA→AVE→AVVP			AVQA→AVVP→AVE		
1	47.41			70.17			70.16		
2	46.54	71.01		69.41	73.04		68.83	48.88	
3	35.66	70.39	72.96	69.49	62.24	48.97	68.93	35.20	71.47

Table 21. Ablation study: Detailed Performance without TMA component under different task orders.

w/o TMA									
Stage	AVE→AVVP→AVQA			AVE→AVQA→AVVP			AVVP→AVE→AVQA		
1	70.47			70.17			49.38		
2	63.31	49.11		70.37	70.01		31.02	69.75	
3	61.00	48.10	69.73	60.42	69.81	49.01	37.08	69.58	69.95
Stage	AVVP→AVQA→AVE			AVQA→AVE→AVVP			AVQA→AVVP→AVE		
1	50.12			70.13			69.56		
2	50.02	69.77		70.05	71.69		69.43	49.75	
3	34.88	69.66	71.19	69.84	60.95	48.69	69.81	30.93	70.67

Table 22. Ablation study: Detailed Performance with D-M-S component ordering under different task orders.

D-M-S									
Stage	AVE→AVVP→AVQA			AVE→AVQA→AVVP			AVVP→AVE→AVQA		
1	51.12			51.82			52.69		
2	31.57	51.17		18.21	63.36		35.89	50.65	
3	14.42	59.29	63.97	26.19	56.71	50.76	43.23	18.31	63.94
Stage	AVVP→AVQA→AVE			AVQA→AVE→AVVP			AVQA→AVVP→AVE		
1	51.72			63.52			63.43		
2	63.10	63.91		58.20	50.03		58.42	53.60	
3	46.90	60.08	51.64	56.67	31.49	50.71	59.41	35.75	51.57

Table 23. Ablation study: Detailed Performance with M-D-S component ordering under different task orders.

M-D-S									
Stage	AVE→AVVP→AVQA			AVE→AVQA→AVVP			AVVP→AVE→AVQA		
1	55.10			54.81			48.60		
2	34.55	52.32		18.07	63.94		31.99	52.84	
3	12.51	63.01	64.52	29.58	58.89	55.21	62.92	19.23	64.51
Stage	AVVP→AVQA→AVE			AVQA→AVE→AVVP			AVQA→AVVP→AVE		
1	50.48			63.22			63.51		
2	63.39	63.97		58.55	52.81		61.02	55.12	
3	37.31	60.97	51.54	61.25	36.42	51.63	61.46	40.29	55.05

Table 24. Ablation study: Detailed Performance with D-S-M component ordering under different task orders.

D-S-M									
Stage	AVE→AVVP→AVQA			AVE→AVQA→AVVP			AVVP→AVE→AVQA		
1	56.72			57.44			51.26		
2	37.76	50.90		16.00	62.67		44.21	56.84	
3	18.98	63.01	54.44	30.67	57.64	53.69	51.10	19.35	63.31
Stage	AVVP→AVQA→AVE			AVQA→AVE→AVVP			AVQA→AVVP→AVE		
1	50.80			54.34			54.44		
2	62.23	64.80		54.34	50.03		54.44	52.96	
3	40.16	61.06	54.18	54.34	31.49	50.94	54.44	38.18	55.72

Table 25. Ablation study: Detailed Performance with M-S-D component ordering under different task orders.

M-S-D									
Stage	AVE→AVVP→AVQA			AVE→AVQA→AVVP			AVVP→AVE→AVQA		
1	55.47			56.39			52.78		
2	39.29	52.13		17.74	62.55		40.80	56.89	
3	15.60	60.53	63.01	22.91	56.70	54.75	61.96	17.71	62.56
Stage	AVVP→AVQA→AVE			AVQA→AVE→AVVP			AVQA→AVVP→AVE		
1	55.12			62.83			62.70		
2	61.40	62.94		62.55	46.07		61.10	53.51	
3	36.53	60.05	53.31	58.27	32.99	54.89	61.12	36.12	51.07

Table 26. Ablation study: Detailed Performance with S-D-M component ordering under different task orders.

S-D-M									
Stage	AVE→AVVP→AVQA			AVE→AVQA→AVVP			AVVP→AVE→AVQA		
1	46.77			48.31			53.01		
2	35.70	53.74		31.52	62.91		32.31	50.32	
3	28.06	53.83	62.70	28.88	60.49	54.20	51.77	30.70	62.95
Stage	AVVP→AVQA→AVE			AVQA→AVE→AVVP			AVQA→AVVP→AVE		
1	52.50			63.60			62.65		
2	56.13	61.54		59.11	45.15		60.05	52.13	
3	28.68	60.64	48.26	61.20	35.77	52.59	59.89	49.47	49.20